Impact of Nanocrystal Spray Deposition on Inorganic Solar Cells

Troy K. Townsend,*,[†] Woojun Yoon, Edward E. Foos, and Joseph G. Tischler

U.S. Naval Research Laboratory, Washington, D.C. 20375, United States

S *Supporting Information*

ABSTRACT: Solution-synthesized inorganic cadmium telluride nanocrystals (~4 nm; 1.45 eV band gap) are attractive elements for the fabrication of thin-film-based low-cost photovoltaic (PV) devices. Their encapsulating organic ligand shell enables them to be easily dissolved in organic solvents, and the resulting solutions can be spray-cast onto indium—tin oxide (ITO)-coated glass under ambient conditions to produce photoactive thin films of CdTe. Following annealing at 380 °C in the presence of $CdCl_{2(s)}$ and evaporation of metal electrode contacts (glass/ITO/CdTe/Ca/Al), Schottky-junction PV devices were tested under simulated 1 sun conditions. An improved PV performance was found to be directly tied to control over the film morphology obtained by the adjustment of spray parameters such as the solution concentration, delivery pressure, substrate distance, and surface temperature. Higher spray pressures produced thinner layers (<60 nm) with lower surface roughness (<200 nm), leading to devices with improved open-circuit voltages (V_{oc}) due to decreased surface roughness and higher short-circuit current (J_{sc}) as a result of enhanced annealing conditions. After process optimization, spray-cast Schottky devices rivaled those prepared by conventional spin-coating, showing $J_{sc} = 14.6 \pm 2.7$ mA cm^{-2}, $V_{oc} = 428 \pm 11$ mV, FF = 42.8 $\pm$ 1.4%, and Eff. = 2.7 $\pm$ 0.5% under 1 sun illumination. This optimized condition of CdTe spray deposition was then applied to heterojunction devices (ITO/CdTe/ZnO/Al) to reach 3.0% efficiency after light soaking under forward bias. The film thickness, surface morphology, and light absorption were examined with scanning electron microscopy, optical profilometry, and UV/vis spectroscopy.
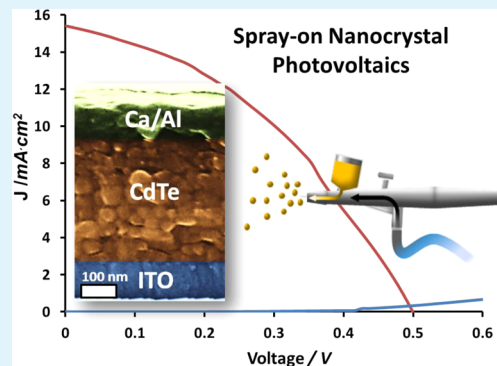
KEYWORDS: *Spray deposition, nanocrystals, CdTe, photovoltaics, solution processing*

The development of inexpensive photovoltaic (PV) technologies may be one of the most important challenges of the century because of the rising demand for global power and the increasing market for creative new device applications.[1] Recent advances in nanoscience have led to inorganic semiconductor materials with unique properties, including synthetically controlled quantum size effects giving rise to tunable band edges for specific optical absorption ranges and heterojunction band-edge energy-level alignments. For these reasons alone, semiconductor nanocrystal "inks" have found applications in a wide array of optoelectronics for active-layer components in solar cells,[2,3] light emitting diodes,[4] photodetectors,[5] photocatalysts,[6−8] and transistors.[9] Similarly, organic semiconductor compounds can be easily deposited from solution; however, they routinely suffer from low thermal and chemical stability and photostability.[10,11] Solution-synthesized inorganic nanocrystals serve to bridge this gap between ideal material properties (e.g., tunable size-dependent band-edge energy levels and inherent stability to heat and oxidation) and low-cost deposition because of their encapsulating solution-compatible ligand shell. In addition, optimization of thin films (in the case of commercial CdTe photovoltaics) has also led to reduced materials and fabrication costs.[12,13] Further studies are needed to weigh the inherent cost reduction of the fabrication and installation for nanocrystal-based photovoltaics with the current lower efficiencies of these emerging technologies. The major challenge for nanocrystal materials will be to optimize solution-processing conditions to achieve comparable device efficiencies. Since the first report on solution processing of colloidal inorganic CdSe/CdTe nanorods by Gur and co-workers,[14] several other groups have produced thin active-layer CdTe nanocrystal films (<500 nm) for solar devices showing as high as 6.9% and 12% efficiency for heterostructures with ZnO[15,16] and up to 5.1% for single-layer Schottky junctions.[17,18] Laboratory spin coating, however, is a less efficient process than spray coating.[19,21] In cases where material costs are high (i.e., custom-synthesized inks or solutions containing rare elements), alternative material deposition technologies are needed.

Spray coating of inorganic materials offers advantages over other solution deposition methods including (1) increased material transfer efficiency of approximately 30% for small substrates,[19] (2) rapid deposition for potential application in roll-to-roll device production, and, most importantly, (3) noncentrifugal-force-directed (i.e., gas-propelled) deposition, enabling production of large area coatings on flexible and irregular surfaces. Despite these advantages, few have studied this spray processing of inorganic nanomaterials with respect to

Scheme 1. Deposition of CdTe Nanocrystals onto ITO Substrates Employing a Layer-by-Layer Method, with SEM Showing Film Cracking on a Single Thick CdTe Top Layer Resulting from the Sintering Process, Including a Device Cross-Sectional SEM Image of a Multilayered ITO/CdTe/Ca/Al Schottky Architecture[a]
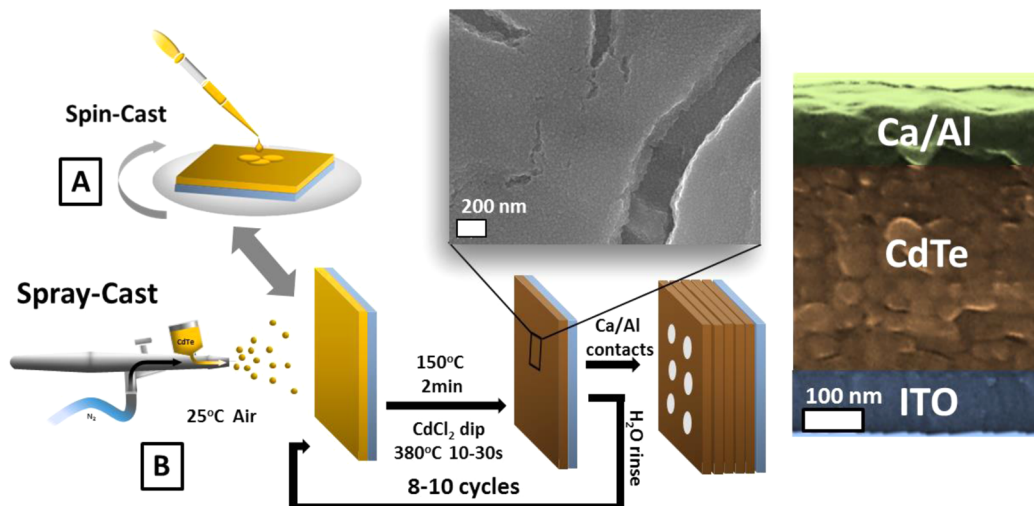
[a]Devices were made either entirely from spin coating (A) or entirely from spray coating (B) of the CdTe material and were both processed in the same manner after deposition.
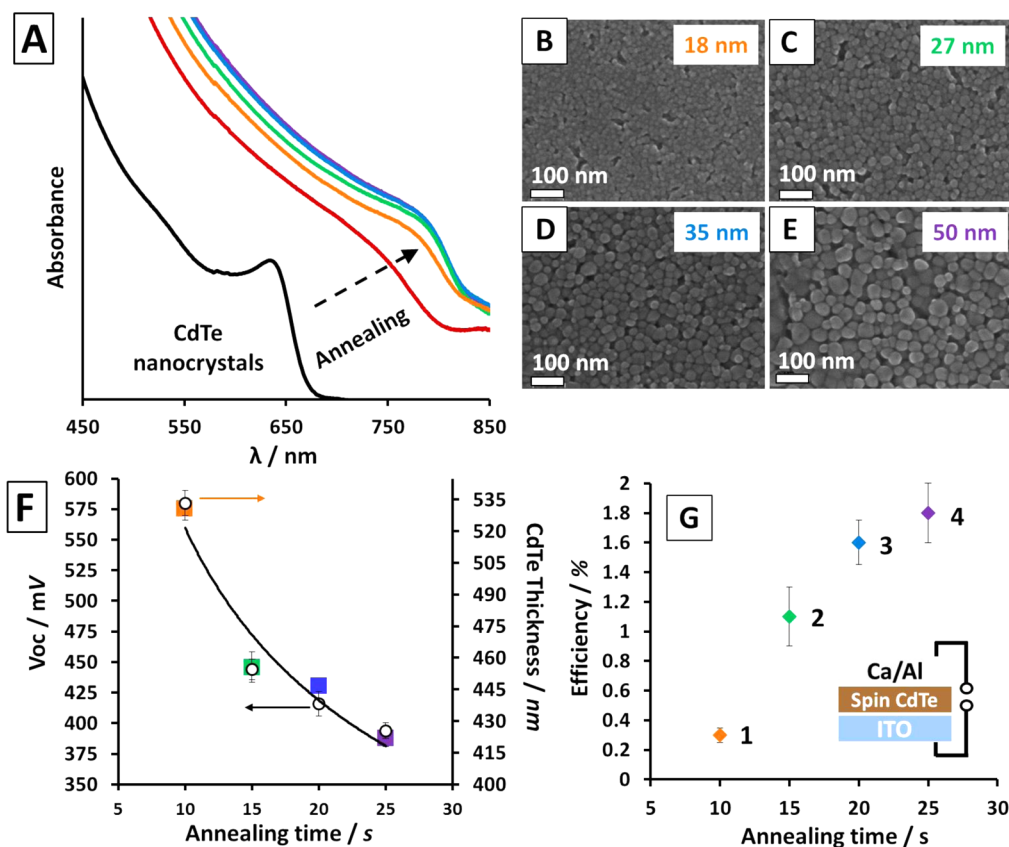

Figure 1. (A) UV/vis absorption of a CdTe nanocrystal solution (black line) and spin-cast CdTe films annealed at 380 °C for 5 s (red line), 10 s (orange line), 15 s (green line), 20 s (blue line), and 25 s (purple line), with SEM images of films treated with increasing annealing times of 10 s (B), 15 s (C), 20 s (D), and 25 s (E) including an average grain size (nm), showing open-circuit voltages (V_{oc}) and the CdTe film thickness as a function of the annealing time (F) and resulting device efficiencies (see Table 1, ID 1−4) as a function of the annealing time and average grain size (G).

photovoltaics with the exception of work on Cu_2ZnSnS_4 (η = 0.23%),[20] CdTe (η = 2.3%),[19,21] $CuInSe_2$ (η = 3.1%),[22,23] and $TiO_2|CuInS_2$ (5.0%).[24] Motivated to optimize spray-coated PV devices from inorganic nanocrystal solutions, in this report we

directed specific focus toward control over spray parameters including the delivery pressure, solution concentration, substrate temperature, and distance from the substrate. From films fabricated in air under ambient conditions, spray-on CdTe
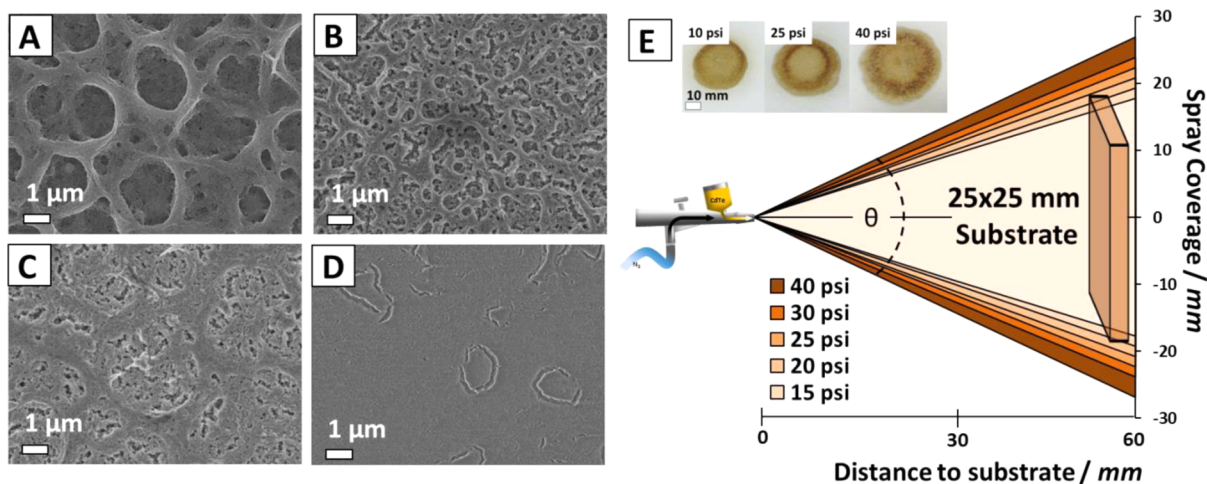
7903

dx.doi.org/10.1021/am501235v | ACS Appl. Mater. Interfaces 2014, 6, 7902−7909

Figure 2. SEM images of sprayed CdTe films under controlled conditions of 30 psi|1 mg mL^{-1}|80 °C (A), 10 psi|1 mg mL^{-1}|80 °C (B), 10 psi|1 mg mL^{-1}|25 °C (C), and 30 psi|4 mg mL^{-1}|25 °C (D) including the spray coverage diameter with pressure plotted as a function of the substrate distance, and images of CdTe films sprayed on paper positioned 60 mm away at 10, 25, and 40 psi (E).

Schottky PV devices were tested under 1 sun illumination and compared to analogous spin-cast films, demonstrating minimal differences in the device performance while emphasizing the importance of an annealing parameter to predict the appropriate annealing time and temperature based on the initial film thickness.

■ RESULTS AND DISCUSSION

Thin films of CdTe nanocrystals (4.1 nm) determined through the use of a published empirical function[25] were spin-cast or spray-cast onto cleaned indium−tin oxide (ITO) glass through an iterative process involving multiple deposition and annealing cycles.[15] This is in contrast with previous reports showing spin coating and sintering of single-layer CdTe nanorods to serve as the active layer.[14,17] Attempts to use nanorods in this study yielded insoluble solutions,[19] whereas spherical nanocrystals were easily dispersed in sprayable solvents. Control of the absorber thickness is required for optimized light absorption, so initially devices were spray-cast and annealed as a single 200−400 nm layer device. However, because of film compression as a result of ligand loss during heating, thick layers of CdTe nanocrystals can generate cracks upon heating, and these gaps in the film can lead to shorter pathways after metal evaporation. To solve this problem, a multilayer assembly[15] was adapted to fill gaps from previous layers, as described in Scheme 1.

Sintering Parameters. In order to accurately investigate the possible effects that methods of processing play on spray-cast CdTe films, a preliminary study on spin-cast films was conducted to first optimize the annealing parameters. This type of process development was previously conducted by Jasieniak and co-workers[15] on spin-coated devices; however, because of the sensitivity of this material to annealing, we discovered that in-laboratory process customization was crucial to accounting for minor differences in the synthesis, environment, and personal techniques. After synthesis and characterization, stock solutions of CdTe nanocrystals were spin-coated onto ITO and annealed in the presence of CdCl$_2$(s) at temperatures between 350 and 400 °C for various amounts of time (10 s to 2 min). Exposure to CdCl$_2$(s) is known to promote CdTe grain growth during annealing, and we found that films annealed at 380 °C for 25 s showed the largest grains (50 ± 15 nm), leading to the highest short-circuit current (J_{sc} =16.1 ± 3.8 mA

cm^{-2}). Larger grains can positively affect charge transport by minimizing surface defects located at the grain boundaries. Longer annealing times produced larger grains, and this was also observed in the UV/vis spectra where absorption onsets red-shifted as crystallite sizes increased (Figure 1A−E). After annealing from 5 to 25 s at 380 °C, we estimated a reduction in the band-gap potential from 1.50 to 1.45 eV from the absorption onsets (Figure 1A). Because of the Bohr-exciton radius of CdTe (∼15 nm),[26] it is not surprising to see incipient quantum confinement effects on grains ranging from 10 to 60 nm, which has also been reported for other semiconductor nanocrystals larger than the Bohr radius.[27]

This result is further supported by a reduction in the open-circuit voltage (V_{oc}) from 580 ± 21 mV for grain diameters of 18 ± 5 nm to 394 ± 13 mV for 50 ± 15 nm grains (Figure 1F). As the quantum-confined nanocrystals approach the properties of bulk-type films upon sintering, the Schottky barrier decreases, leading to lower photovoltages. This was found to be true for size-controlled PbS and PbSe nanocrystal Schottky solar cells where quantum confinement was found to determine band-edge energy-level alignments at the semiconductor/metal interface.[28,29] However, this change in the band gap does not account for the total decrease in the observed V_{oc}, which is most likely a result of higher densities of midgap trap states, which were previously found to increase with longer sintering times.[30] We also observed a strong relationship between the film thickness and open-circuit voltages (Figure 1F). As would be expected, longer sintering times promoted consolidation of the nanocrystal grains, causing a reduction in the volume of the film. Interestingly, an increased packing density was found to scale directly with open-circuit voltages at longer annealing times. A decrease of 186 mV was observed for annealing times of 10−25 s, and this also correlates with a film compression of 108 nm (Figure 1F). Despite the observed drop in the voltage, device efficiencies continued to improve with longer annealing times because of an interplay with increasing current density, giving rise to devices showing ∼2.0% efficiency under 1 sun illumination, as shown in Figure 1G. However, annealing beyond 30 s produced devices with lower efficiencies, forming smaller, less discrete grains, which we believe to be decomposition of the residual organic residue from the original
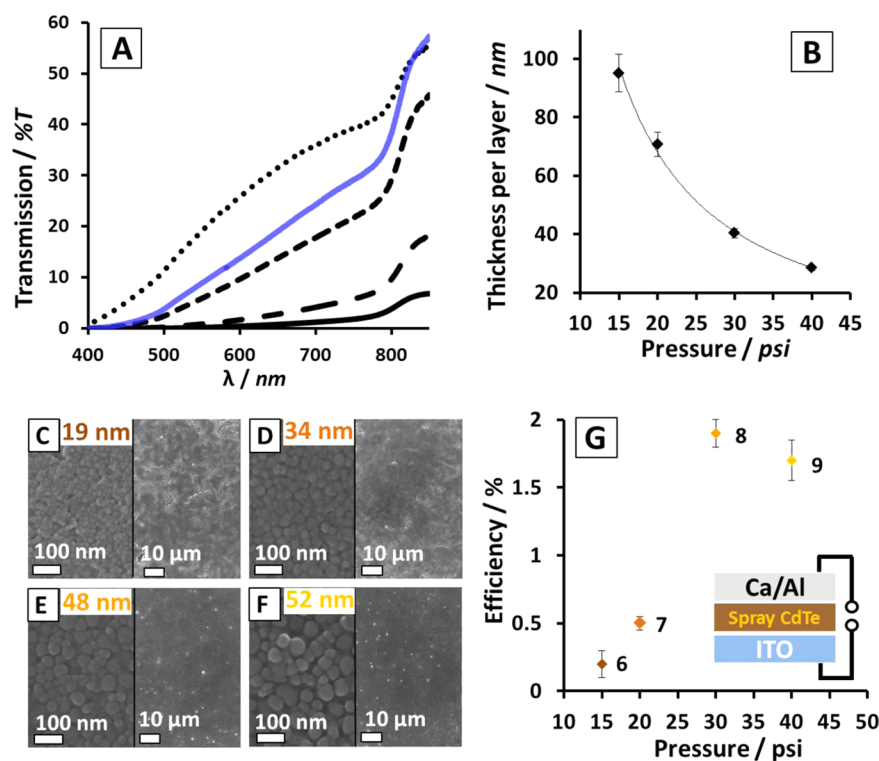
Figure 3. (A)Transmission of light through CdTe device films (as optimized from Figure 2D) annealed at 380 °C for 25 s after spray-cast deposition at 10 (—), 20 (— —), 30 (- - -), and 40 psi (···) with a spin-cast device (blue —) for comparison. (B) Average film thickness as a function of the spray pressure. SEM images split with low magnification of CdTe device films spray-cast at 10 (C), 20 (D), 30 (E), and 40 psi (F) including the average grain size (nm) and device efficiencies (see Table 1, ID 6−9, for other data including rms surface roughness values) as a function of the pressure (G). Optical profilometry scans of these films are also given in Figure S2 in the SI.

oleate ligands, as identified from Fourier transform infrared spectra from preannealed films.[15]

Spray Processing. Unlike spin coating, which routinely produces uniform smooth films, the spray process has the potential to fabricate wide varieties of surface roughness features. We found that the film structure is highly sensitive to spray parameters and that careful control over the pressure, concentration, and distance can lead to smooth films [>20 nm root-mean-square (rms) roughness] or rough films (>200 nm), as shown in Figure 2A−D. Increased light scattering from the "webbed" nanocrystal films (metallic or semiconductor materials) sprayed with high pressure/low concentration/ heated substrate (Figure 2A) could have applications in solar cells, plasmonics, or other light-trapping technologies. Additionally, sprayable high-surface-area inorganic semiconductor scaffolds for catalysis reactions would also be interesting to explore for this unique route toward template-free semiconductor frameworks.[31]

In our previous report on sprayed CdTe PV devices, however, increased leakage current (dark current) was found to be a result of the higher surface roughness topography.[19] This led to a reduction in the open-circuit voltage because of increased surface contact resistance with the metal at the Schottky junction. Higher contact area can play an important role in the device performance especially considering that the roughness (200 nm) is on the order of the film thickness (510 nm). In addition to the introduction of shunting pathways in patches where the film is thinner, higher surface roughness also raises the probability of surface defects and trap states, leading to increased recombination.[30] Motivated to improve V_{oc} by refining the semiconductor/metal interface, we were able to

produce smooth films with roughness values as low as 20 nm (Figure 2D). The best devices were made from the spraying of concentrated CdTe nanocrystal solutions (4 mg mL^{-1}) at high pressures (20−40 psi) at room temperature and short distances (30−60 mm) to reduce the rate of drying. This eliminated the webbed structure that we initially observed, which was attributed to rapid solvent drying upon contact with the heated substrate, forming a coffee ring structure of solid nanocrystals around the 1−3 μm aerosolized droplets (Figure 2A). This rough morphology was observed in our previous report on sprayed films and resembled Figure 2B as a result of spraying at low pressures and concentrations.[19]

After a reduction of the spray-cast film surface roughness, fine-tuning of the spray pressure was used to adjust the layer thickness. This adjustment was found to ultimately affect the degree of cracking and grain growth upon annealing. As depicted in Figure 2E, the spray coverage area increased by >50% as the nozzle pressure increased from 15 to 40 psi. Because the same amount (0.25 mL, 4 mg mL^{-1}) of CdTe is sprayed for each pressure (15, 20, 25, 30, and 40 psi), the volume of material transfer decreases with increasing pressure as the spray diameter becomes larger than the small 25 × 25 mm^2 ITO substrate. As a result, thinner CdTe films are deposited at higher pressures. This becomes apparent in the optical transmission spectra (low light penetration for optically dense films sprayed at lower pressures; Figure 3A) and is further verified by optical profilometry measurements (Figures 3B and S2 in the Supporting Information, SI). Upon calculation of the mass of CdTe present in solution compared to the mass deposited on a substrate, we estimate 15−30% transfer efficiencies for these small substrates because of material lost

Table 1. Summary of the PV Performance of a Metal (Ca/Al)/CdTe Nanocrystal Schottky Junction and (Al)-ZnO/CdTe Heterojunction Solar Cells in the under AM1.5G-Filtered Spectral Illumination (100 mW cm^{-2})[a]

deposition	ID	concn (mg mL^{-1})	layers/cycles	annealing (s)	annealing parameter (°C s nm^{-1})	CdTe thickness (nm)	rms roughness (nm)	J_{sc} (mA cm^{-2})	V_{oc} (mV)	FF (%)	Eff. (%)
spin-coated Schottky	1	40	8	10	57	530 ± 10	41 ± 18	1.4 ± 0.1	580 ± 21	40.8 ± 2.3	0.3 ± 0.1
	2	40	8	15	100	456 ± 14	29 ± 15	7.1 ± 1.0	444 ± 17	33.7 ± 3.5	1.1 ± 0.4
	3	40	8	20	136	447 ± 4	51 ± 16	11.5 ± 1.1	416 ± 20	33.1 ± 3.2	1.6 ± 0.3
	4	40	8	25	180	422 ± 8	57 ± 21	12.1 ± 1.9	394 ± 13	37.8 ± 2.2	1.8 ± 0.4
	5	35	7	25	267	249 ± 22	22 ± 12	16.1 ± 3.8	356 ± 9	36.7 ± 7	2.2 ± 0.8

deposition	ID	concn (mg mL^{-1})	layers/cycles	pressure (psi)	annealing parameter (°C s nm^{-1})	CdTe thickness (nm)	rms roughness (nm)	J_{sc} (mA cm^{-2})	V_{oc} (mV)	FF (%)	Eff. (%)
spray-coated Schottky	6	4	10	15	100	951 ± 128	268 ± 45	1.1 ± 1.0	473 ± 35	33.6 ± 5.2	0.2 ± 0.2
	7	4	10	20	134	707 ± 82	173 ± 29	2.9 ± 0.8	517 ± 15	33.4 ± 4.3	0.5 ± 0.1
	8	4	10	30	235	403 ± 31	50 ± 24	10.5 ± 0.8	447 ± 16	40.4 ± 2.5	1.9 ± 0.2
	9	4	10	40	333	285 ± 18	22 ± 12	9.1 ± 1.0	476 ± 10	38.9 ± 0.3.4	1.7 ± 0.3
	10	3.5	10	30	594	160 ± 12	25 ± 11	12.7 ± 0.4	382 ± 20	45.8 ± 0.7	2.2 ± 0.1
	11	3.5	12	30	579[b]	394 ± 9	67 ± 9	12.7 ± 1.6	392 ± 23	42.4 ± 1.9	2.1 ± 0.3
	12	3.5	24	30	938[b]	243 ± 39	51 ± 14	14.6 ± 2.7	428 ± 11	42.8 ± 1.4	2.7 ± 0.5
spray-coated heterojunction	13	3.5	12	30	560[b]	407 ± 21	61 ± 13	15.3 ± 0.6	479 ± 17	41.4 ± 2.4	3.0 ± 0.2

[a]The device area is 0.1 cm^2. [b]Annealing parameter set to 235 °C s nm^{-1}; however, this artificially increased because of the increased packing density of the film upon annealing.

behind the 6.45 cm^2 substrate as a result of the 18−27 mm spray diameter. However, it is worth noting that spraying onto large surfaces should improve this efficiency as the surface-to-edge area ratio of the substrate increases. Upon sintering, film compression occurs as a result of the high-surface-area nanocrystals consolidating into larger grains (vide supra or Figure 1). This effect was found to be more pronounced in thicker films, leading to the formation of layer cracking at low pressures; however, this was mitigated at higher pressures (Figure 3C−F). This reduction in the degree of cracking also helped to contribute to lower roughness (Table 1).

On the basis of annealing optimization for ~40-nm-thick spin-coated layers, we found that heating at 380 °C for 25 s produced the best devices with large grains (Figure 1E). Interestingly, however, when this annealing was applied to spray-coated films, the grain sizes remained small for low spray pressures but increased for high pressures. Figure 3G shows an increase in the efficiency from devices sprayed at 15 psi (951 nm thick) to 0.2 ± 0.2%, whereas that for devices sprayed at 30 psi (403 nm thick) was 1.9 ± 0.2% (a factor of 9.5 improvement). This arises as a result of annealing of these films for the same amount of time despite their differences in thickness. Because of the higher heat per volume of the thin layers, grain sizes grew faster as J_{sc} increased from 1.1 ± 1.0 to 10.5 ± 0.8 mA cm^{-2} (Figure 3C−F and Table 1). This result points to the important observation that optimized annealing conditions depend strongly on the initial layer thickness (i.e., that thicker CdTe layers require more heat to sinter). This is surprising considering the diminutive thickness of these layers (30−100 nm) and underscores the sensitivity of this material to annealing conditions. On the basis of the thickness of films sprayed at 30 psi (40 nm per layer) and the annealing conditions of 380 °C for 25 s, we estimate an optimal heating rate per layer thickness of CdTe nanocrystals for the best spray device of 235 °C s nm^{-1}, which is in good agreement with a comparable spin-coated device showing 267 °C s nm^{-1}. Because it incorporates the thickness, this parameter may be

used to predict the optimal annealing temperature and time for a given film despite its thickness. To further test how this "annealing parameter" affects the grain size and device performance, multilayer thin CdTe films (40 nm per layer) were sprayed and annealed for 25 s at 380 °C (235 °C s nm^{-1}). Likewise, a separate film was sprayed with double the thickness (80 nm per layer) and treated with double the annealing time for 50 s at 380 °C, also 235 °C s nm^{-1} (annealing time of 50 s = 235 °C s nm^{-1} × 80 nm × 380 °C^{-1}) according to the hypothesis that these films should show comparable grain growth. Indeed, the scanning electron microscopy (SEM) images of the two films revealed similar grain sizes and support the use of an annealing parameter to control grain growth in nanocrystalline films with varied thicknesses. Figure S1 in the SI shows these SEM images and a plot of the device efficiencies as a function of the annealing parameters.

Device Structures. Following the optimization steps, we turned our attention to device fabrication. In an attempt to preserve the high J_{sc} values (as a result of larger grains from thinner layers), while also raising the V_{oc} (thicker spin-coated films produced higher V_{oc} values), spray-cast Schottky junction devices were fabricated with 24 deposition cycles (2.4 times more) while maintaining 235 °C s nm^{-1}. In parallel, to validate the usage of the annealing parameter on the device performance, a second device was fabricated with 12 cycles of layers twice as thick (also 235 °C s nm^{-1}) but annealed for 50 s. These two devices showed comparable grain sizes (Figure S1 in the SI) and PV performance (Table 1, ID 12 and 13), further pointing toward the importance of optimized thickness-dependent annealing parameters for nanocrystal CdTe films. These thicker films also produced devices with the highest efficiencies because of increased light absorption and charge-carrier generation while maintaining high open-circuit voltages, showing device efficiencies ranging between 2.2% and 3.2%. This variability comes as a result of the range in the short-circuit current density from 12 to 17 mA cm^{-2}, which suggests some degree of nonuniformity of the sprayed film thickness.
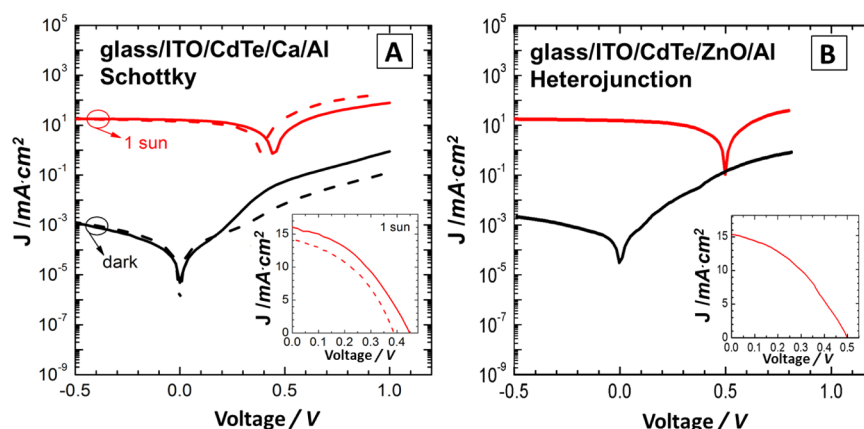
Figure 4. Current–voltage curves under 1 sun simulated sunlight (red) and in the dark (black) for representative 0.1 cm² spray-coated (—) and spin-coated (- - -) Schottky devices (A) and spray-coated heterojunction devices after 30 min of light soaking with forward bias (details in the SI; B).

Thickness variations like this occur because of the nature of the hand-held airbrush; however, mechanical automation of the spray process may improve the film regularity. Notably, the best sprayed films resembled spin-coated films because of lower surface roughness morphology, which led to increased open-circuit voltages as a result of minimized leakage current (Figure 4A) compared to our previous spray-cast devices with higher surface roughness, which displayed 2 orders of magnitude higher saturation dark-current density prior to optimization.[19]

Taking advantage of their simplicity, single-layer CdTe Schottky devices were used to optimize spray-processing conditions. However, because of the limited shelf-life of the reactive calcium metal contact in air, more stable device structures were explored. Following the work of Jasieniak and colleagues on spin-coated structures, spray-cast CdTe devices were fabricated with an n-type ZnO hole blocking layer and capped with an aluminum contact.[15] These devices were found to be stable in air and led to enhanced performance (Table 1 and Figure 4B). On the basis of a report by Panthani et al., treating the devices with light soaking under forward bias improves the PV performance by altering the nature of the ITO/CdTe interface.[16] The mechanism for this process remains unknown and deserves further investigation, especially considering our devices observed signs of reversal when stored in the dark for 2 weeks. The effects of this treatment are shown in Table S1 and Figure S3 in the SI, where devices were exposed to 5 min doses of 3.0 V forward bias under 1 sun illumination between measurements. This led to an increase in the efficiency from 2.4 to 3.0% largely because of increasing V_{oc} values.

CONCLUSIONS

In summary, we have produced spray-cast CdTe films under ambient conditions for all-inorganic Schottky barrier PV devices (illuminated under AM1.5G simulated sunlight; $\eta >$ 2%) with properties that are virtually equivalent to those of conventional spin-cast CdTe devices. A transition from quantum-confined nanocrystals to bulk-like films accompanied film compression during annealing and was found to scale indirectly with open-circuit voltages. This affect, however, was overshadowed by increasing short-circuit current densities as a result of grain growth. After optimization of the spray process to produce smooth dense nanocrystal films, thinner layers were observed with increased spray pressure, resulting in fewer cracks and more heat per annealed layer, improving the J_{sc}

values. The thickness dependence of the annealing parameter for films sprayed at different pressures became apparent because layers sprayed at low pressures (thick) required more heat to complete annealing than layers sprayed at high pressures (thin). After the optimal spray-casting and annealing conditions were determined, spray Schottky devices were found to have the highest performance with efficiencies between 2.2% and 3.2%. This spray process was also applied to produce CdTe films for an air-stable ITO/CdTe/ZnO/Al heterostructure, which was further improved with light soaking under forward bias, producing spray-cast devices with 3.0% efficiency. Spray-on nanocrystal solutions have unique advantages of deposition compared to other methods (spin, dip, drop-coating, etc.) including fewer limitations on equipment costs, lower energy requirements, and higher material transfer efficiencies. The added deposition freedoms inherent to spray coating also promote the capability to coat large and irregular surfaces, inspiring new and imaginative applications for next-generation solar cells and optoelectronics.

EXPERIMENTAL SECTION

Nanocrystal Synthesis. All reactions were conducted under inert conditions using standard Schlenk techniques unless otherwise noted. Oleic acid (90%), 1-octadecene (90%), trioctylphosphine (TOP; 90%), and selenium (99.5+%) were purchased from Aldrich. CdO (99.99%) and tellurium (99.8%) were purchased from Strem. All reagents were used as received except for pyridine, which was purified through distillation. The CdTe nanocrystals were synthesized according to a published procedure.[15] Briefly, 0.48 g of CdO and 4.29 g of oleic acid were mixed with 76 mL of 1-octadecene and evacuated at 100 °C for 20 min. Under an argon atmosphere, this solution was brought to 360 °C. Separately, 0.24 g of tellurium in 4.34 g of TOP were prepared and loaded into a syringe followed by an additional 5 g of 1-octadecene. Quickly, the heating mantle was removed from the cadmium solution, and the Te-TOP solution was injected into the headspace above the reaction, which was allowed to cool naturally to 30 °C. Following isolation from the reaction, the solid was dissolved in 5 mL of pyridine and transferred to a round-bottomed flask and the solution lowered into a 85 °C heating mantle and stirred overnight. The dark-reddish-brown solid (~400 mg) was precipitated with 40 mL of hexanes, isolated by a centrifuge (3900 rpm; 2 min), and redissolved in 10 mL of 1:1 (v/v) pyridine/1-propanol. The concentration of the CdTe stock solution was determined to be 40 mg mL⁻¹ by evaporation. ZnO sol–gel solutions were prepared by mixing monoethanolamine and zinc acetate hydrate (1:1 molar ratio of 0.5 M each) in 2-methoxyethanol and heating at 60 °C for 90 min following a literature procedure.[32]

Device Fabrication. All device samples were fabricated in air on ITO-coated (sheet resistance of 8−12 Ω □$^{-1}$) glass substrates (25 × 25 × 0.7 mm^3) obtained from Delta Technologies. The substrates were sonicated separately in acetone and ethanol, dried under a stream of dinitrogen, and cleaned via UV/ozone (12 min; 150 °C; 0.5 L min^{-1} flow rate) immediately prior to film deposition. The spin-coating procedure was conducted as reported in the literature using the 40 mg mL^{-1} stock solution.[15,33]

Spray Process. For spray-coated samples, 6.45 cm^2 substrates were mounted vertically with tape. The spray solution (diluted to 4 mg mL^{-1} in CHCl$_3$) was loaded into a gravity-fed Paasche VSR90#1 airbrush equipped with a 0.254 mm needle and one velocity setting. The nanocrystals were applied uniformly using a rapid side-to-side passing spray perpendicular to the substrate at a distance of 60 mm from the spray nozzle.[19,21] The spray pressure of dinitrogen carrier gas was controlled with a regulator and varied between 10 and 40 psi. The duration of spray per layer varied with pressure from 3 to 5 s for a 0.25 mL deposition. After one layer (0.25−0.5 mL) had been deposited, the substrate was removed from the sample mount and processed as follows to complete one processing cycle per layer. After nanocrystal deposition (spin or spray coating), the film was dried on a 150 °C hot plate for 2 min, immersed in a saturated solution of CdCl$_2$ in methanol warmed to 60 °C for 5 s, and then dipped in isopropyl alcohol for 3 s and blown dry with dinitrogen to remove excess CdCl$_2$. To induce sintering, films were annealed on a 380 °C hot plate in air for 10−50 s. After cooling to room temperature, the sample was rinsed with water, dried, and remounted and the procedure repeated for 7−24 cycles. Completed CdTe films were exposed to air for several days without special effort to store under inert conditions prior to metal evaporation.

Device Construction. Following material deposition through either spin or spray coating, Schottky devices (ITO/CdTe/Ca/Al) were completed via a sequential thermal evaporation of calcium (20 nm) and aluminum (80 nm), whereas heterojunction devices (ITO/CdTe/ZnO/Al) were capped only with aluminum (130 nm). Shadow masks were used to define the active area of each cell to 0.10 cm^2. ZnO layers were formed by spin coating the zinc acetate precursor solution at 2000 rpm for 30 s four times to form approximately 60 nm of ZnO on top of the CdTe film and then annealing at 300 °C for 2 min.

Device Characterization. The film morphology, thickness, and surface roughness were determined with a Leo 1550 scanning electron microscope and a Zygo optical profilometer. The current density− voltage (*J*−*V*) characteristics of the Schottky devices were measured with a semiconductor parameter analyzer (Keithley 4200) and an Oriel PVIV-1A Test Station for the heterostructures. The solar cell efficiency was measured under the spectral output from a 150 W solar simulator (Newport Corp., Springfield, OH) using an air mass 1.5 global (AM 1.5G) filter. The irradiance (100 mW cm^{-2}) of the solar simulator was adjusted using a reference cell 91150 V (Newport Corp., Springfield, OH) and a 818-SL-L silicon photodetector standard (Newport Corp., Springfield, OH) that has been cross-calibrated by a reference silicon cell traceable to the National Renewable Energy Laboratory.

ASSOCIATED CONTENT

Ⓢ Supporting Information
Details of the annealing parameter as a function of the PV device efficiency, optical profilometry of spin-coated and spray-cast CdTe devices, and PV response of light soaking on sprayed PV devices. This material is available free of charge via the Internet at http://pubs.acs.org.

AUTHOR INFORMATION

Corresponding Author
*E-mail: troy.townsend.ctr@nrl.navy.mil.
Author Contributions
The manuscript was written through contributions of all authors. All authors have given approval to the final version of the manuscript. All authors contributed equally.

Notes

ACKNOWLEDGMENTS

REFERENCES

(1) Lewis, N. S. Powering the Planet. *MRS Bull.* **2007**, *32*, 808−820.
(2) Debnath, R.; Bakr, O.; Sargent, E. H. Solution-Processed Colloidal Quantum Dot Photovoltaics: A Perspective. *Energy Environ. Sci.* **2011**, *4*, 4870−4881.
(3) Tang, J.; Sargent, E. H. Infrared Colloidal Quantum Dots for Photovoltaics: Fundamentals and Recent Progress. *Adv. Mater.* **2011**, *23*, 12−29.
(4) Demir, H. V.; Nizamoglu, S.; Erdem, T.; Mutlugun, E.; Gaponik, N.; Eychmüller, A. Quantum Dot Integrated LEDs using Photonic and Excitonic Color Conversion. *Nano Today* **2011**, *6*, 632−647.
(5) Konstantatos, G.; Sargent, E. H. Nanostructured Materials for Photon Detection. *Nat. Nanotechnol.* **2010**, *5*, 391−400.
(6) Frame, F. A.; Townsend, T. K.; Chamousis, R. L.; Sabio, E. M.; Dittrich, T.; Browning, N. D.; Osterloh, F. E. Photocatalytic Water Oxidation with Nonsensitized IrO$_2$ Nanocrystals under Visible and UV Light. *J. Am. Chem. Soc.* **2011**, *133*, 7264−7267.
(7) Holmes, M. A.; Townsend, T. K.; Osterloh, F. E. Quantum Confinement Controlled Photocatalytic Water Splitting by Suspended CdSe Nanocrystals. *Chem. Commun.* **2012**, *48*, 371−373.
(8) Townsend, T. K.; Sabio, E. M.; Browning, N. D.; Osterloh, F. E. Photocatalytic Water Oxidation with Suspended Alpha-Fe$_2$O$_3$ Particles—Effects of Nanoscaling. *Energy Environ. Sci.* **2011**, *4*, 4270−4275.
(9) Ridley, B. A.; Nivi, B.; Jacobson, J. M. All-Inorganic Field Effect Transistors Fabricated by Printing. *Science* **1999**, *286*, 746−749.
(10) Lee, J. U.; Jung, J. W.; Jo, J. W.; Jo, W. H. Degradation and Stability of Polymer-Based Solar Cells. *J. Mater. Chem.* **2012**, *22*, 24265−24283.
(11) Jørgensen, M.; Norrman, K.; Krebs, F. C. Stability/Degradation of Polymer Solar Cells. *Sol. Energy Mater. Sol. Cells* **2008**, *92*, 686−714.
(12) Zweibel, K. Issues in Thin Film PV Manufacturing Cost Reduction. *Sol. Energy Mater. Sol. Cells* **1999**, *59*, 1−18.
(13) Zweibel, K. Thin Film PV Manufacturing: Materials Costs and their Optimization. *Sol. Energy Mater. Sol. Cells* **2000**, *63*, 375−386.
(14) Gur, I.; Fromer, N. A.; Geier, M. L.; Alivisatos, A. P. Air-Stable All-Inorganic Nanocrystal Solar Cells Processed from Solution. *Science* **2005**, *310*, 462−465.
(15) Jasieniak, J.; MacDonald, B. I.; Watkins, S. E.; Mulvaney, P. Solution-Processed Sintered Nanocrystal Solar Cells via Layer-by-Layer Assembly. *Nano Lett.* **2011**, *11*, 2856−2864.
(16) Panthani, M. G.; Kurley, J. M.; Crisp, R. W.; Dietz, T. C.; Ezzyat, T.; Luther, J. M.; Talapin, D. V. High Efficiency Solution Processed Sintered CdTe Nanocrystal Solar Cells: The Role of Interfaces. *Nano Lett.* **2013**, *14*, 670−675.
(17) Olson, J. D.; Rodriguez, Y. W.; Yang, L. D.; Alers, G. B.; Carter, S. A. CdTe Schottky Diodes from Colloidal Nanocrystals. *Appl. Phys. Lett.* **2010**, *96*, 242103.
(18) Sun, S.; Liu, H.; Gao, Y.; Qin, D.; Chen, J. Controlled Synthesis of CdTe Nanocrystals for High Performanced Schottky Thin Film Solar Cells. *J. Mater. Chem.* **2012**, *22*, 19207−19212.
(19) Foos, E. E.; Yoon, W.; Lumb, M. P.; Tischler, J. G.; Townsend, T. K. Inorganic Photovoltaic Devices Fabricated Using Nanocrystal Spray Deposition. *ACS Appl. Mater. Interfaces* **2013**, *5*, 8828−8832.
(20) Steinhagen, C.; Panthani, M. G.; Akhavan, V.; Goodfellow, B.; Koo, B.; Korgel, B. A. Synthesis of Cu$_2$ZnSnS$_4$ Nanocrystals for Use in Low-Cost Photovoltaics. *J. Am. Chem. Soc.* **2009**, *131*, 12554−12555.

(21) Javier, A.; Foos, E. E. Nanocrystal Photovoltaic Paint Sprayed with a Handheld Airbrush. *IEEE Trans. Nanotechnol.* **2009**, *8*, 569−573.

(22) Akhavan, V. A.; Goodfellow, B. W.; Panthani, M. G.; Reid, D. K.; Hellebusch, D. J.; Adachi, T.; Korgel, B. A. Spray-Deposited CuInSe$_2$ Nanocrystal Photovoltaics. *Energy Environ. Sci.* **2010**, *3*, 1600−1606.

(23) Akhavan, V. A.; Panthani, M. G.; Goodfellow, B. W.; Reid, D. K.; Korgel, B. A. Thickness-Limited Performance of CuInSe$_2$ Nanocrystal Photovoltaic Devices. *Opt. Express* **2010**, *18*, A411−A420.

(24) Nanu, M.; Schoonman, J.; Goossens, A. Nanocomposite Three-Dimensional Solar Cells Obtained by Chemical Spray Deposition. *Nano Lett.* **2005**, *5*, 1716−1719.

(25) Yu, W. W.; Qu, L.; Guo, W.; Peng, X. Experimental Determination of the Extinction Coefficient of CdTe, CdSe, and CdS Nanocrystals. *Chem. Mater.* **2003**, *15*, 2854−2860.

(26) Masumoto, Y.; Sonobe, K. Size-Dependent Energy Levels of CdTe Quantum Dots. *Phys. Rev. B* **1997**, *56*, 9734−9737.

(27) Townsend, T. K.; Browning, N. D.; Osterloh, F. E. Nanoscale Strontium Titanate Photocatalysts for Overall Water Splitting. *ACS Nano* **2012**, *6*, 7420−7426.

(28) Yoon, W.; Boercker, J. E.; Lumb, M. P.; Placencia, D.; Foos, E. E.; Tischler, J. G. Enhanced Open-Circuit Voltage of PbS Nanocrystal Quantum Dot Solar Cells. *Sci. Rep.* **2013**, *3*, 1−7.

(29) Choi, J. J.; Lim, Y.-F.; Santiago-Berrios, M. E. B.; Oh, M.; Hyun, B.-R.; Sun, L.; Bartnik, A. C.; Goedhart, A.; Malliaras, G. G.; Abruña, H. c. D.; Wise, F. W.; Hanrath, T. PbSe Nanocrystal Excitonic Solar Cells. *Nano Lett.* **2009**, *9*, 3749−3755.

(30) Bezryadina, A.; France, C.; Graham, R.; Yang, L.; Carter, S. A.; Alers, G. B. Mid-Gap Trap States in CdTe Nanoparticle Solar Cells. *Appl. Phys. Lett.* **2012**, *100*, 013508−1−013508−4.

(31) Yang, M.; DiSalvo, F. J. Template-Free Synthesis of Mesoporous Transition Metal Nitride Materials from Ternary Cadmium Transition Metal Oxides. *Chem. Mater.* **2012**, *24*, 4406−4409.

(32) Saleem, M.; Fang, L.; Wakeel, A.; Rashad, M.; Kong, C. Simple Preparation and Characterization of Nano-Crystalline Zinc Oxide Thin Films by Sol-Gel Method on Glass Substrate. *World J. Condens. Matter Phys.* **2012**, *2*, 10−15.

(33) Yoon, W.; Foos, E. E.; Lumb, M. P.; Tischler, J. G. Solution processing of CdTe nanocrystals for thin-film solar cells. *38th IEEE Photovoltaic Spec. Conf.* **2012**, 002621−002624.